Phys. Status Solidi B **253,** No. 10, 1916–1922 (2016) / **DOI** 10.1002/pssb.201600152

physica status solidi b
www.pss-b.com
basic solid state physics

Phonon-assisted tunnel emission of holes from the double donor level of the EL2 defect

Tadeusz Wosinski*

Institute of Physics, Polish Academy of Sciences, Al. Lotnikow 32/46, 02-668 Warsaw, Poland

Received 24 March 2016, revised 16 May 2016, accepted 20 May 2016
Published online 10 June 2016

Keywords charge carrier emission, deep levels, defects, GaAs, phonons, tunnel ionisation

* e-mail wosin@ifpan.edu.pl, Phone: +48 22 843 7001, Fax: +48 22 843 0926

Strong electric-field-induced enhancement of the thermal emission rate of holes from the doubly ionised charge state of the EL2 defect was revealed with the double-correlation deep-level transient spectroscopy in p-type GaAs crystals of various crystallographic orientations. The observed enhancement, by over four orders of magnitude of the emission rate, was analysed in a model of phonon-assisted tunnel ionisation. Similar dependences of the hole-emission rate on the electric-field intensity received for the electric-field directions parallel to three main crystallographic axes evidence for tetrahedral symmetry of the defect, which is consistent with its identification as the isolated arsenic antisite defect.

1 Introduction Group III–V compound semiconductors, such as GaAs, InAs and their ternary alloys, which combine unique optical and electronic properties, are widely used in opto-electronic devices for optical communications as well as in high-speed and -frequency electronic systems. Because of their excellent electron transport properties and the level of maturity reached in processing, those III–V semiconductors offer also a promising alternative for replacing silicon as the channel material in metal–oxide–semiconductor (MOS) devices for modern logic circuits [1]. A crucial feature in successful MOS application is the high quality of the semiconductor/oxide interface. This becomes a real challenge for the III–V semiconductors, which suffer from the poor quality of the interface with their native oxides, containing a large density of interfacial traps leading to strong Fermi-level pinning. Identification of the microscopic nature of defects responsible for those traps and control of their densities are of fundamental importance. Both the recent theoretical calculations through hybrid density functionals [2] and the experimental study using electron paramagnetic resonance (EPR) [3] point to arsenic antisite defects, As atom on Ga site As_{Ga}, as the most probable constituent of the electrically active traps observed at the GaAs/oxide and InGaAs/oxide interfaces.

Already three decades earlier the arsenic antisite defect, of tetrahedral T_d symmetry, was identified, on the basis of photo-EPR measurements of GaAs crystals under monochromatic light illumination [4] and, independently, on the grounds of melt stoichiometry dependence of deep-level trap densities in Bridgman grown GaAs crystals determined with deep-level transient spectroscopy (DLTS) [5], as the defect responsible for the dominant deep-level electron trap in melt-grown GaAs crystals, known as EL2. However, the microscopic nature of this technologically important defect, responsible for Fermi-level pinning at the mid-gap and the semi-insulating behaviour of undoped GaAs, is still controversial [3].

Several other defects, containing As_{Ga} as a constituent, were considered to account for the unusual optical properties of the EL2 trap associated with its optically induced transition to a metastable excited state. The first one was the $(As_{Ga})_2$ dimer composed of two nearest-neighbour As_{Ga} defects, representing an orthorhombic defect of C_{2v} symmetry, proposed by Figielski et al. [6, 7]. However, later detailed piezospectroscopic studies of splittings, under uniaxial stress applied along the main crystallographic directions, of the zero-phonon line in the EL2-related optical absorption pointed to tetrahedral symmetry of the local crystal field around the EL2 defect, ruling out its C_{2v} symmetry [8]. Another defect proposed for the origin of the EL2 trap was an arsenic–antisite–arsenic–interstitial, As_{Ga}–As_i, pair of trigonal C_{3v} symmetry. This identification

was based on the results of optically detected electron-nuclear double resonance (ODENDOR) experiments [9, 10] and on the observed evolution of the EL2-related DLTS spectrum in GaAs Schottky diode subjected to annealing under reverse bias conditions [11], which was later questioned in view of results of similar independent experiments [12]. Moreover, the observed stability of the EL2 defect in GaAs crystals subjected to a high-intensity ultrasonic vibration [13] was in contradiction with its identification as the weakly bonded As_{Ga}–As_i pair.

Nevertheless, several further studies, by means of the optically detected EPR and ODENDOR methods, reported in an extensive review article by Koschnick and Spaeth [14], pointed to the As_{Ga}–As_i pair as the most probable origin of the EL2 defect. Even more complicated, three-centre-complex defect, composed of As_{Ga}, Ga_{As} (gallium antisite) and V_{As} (arsenic vacancy), was proposed by Fukuyama et al. [15] to account for the properties of both the normal and metastable states of the EL2 defect. However, systematic investigations of energy levels related to EL2 in its normal and metastable states in semi-insulating GaAs crystals, using a number of spectroscopic techniques, like photocurrent, thermally stimulated current, photo-Hall effect and thermally stimulated Hall effect, did not allow to distinguish unambiguously between that three-centre complex and the isolated As_{Ga} antisite models of the EL2 defect [16]. Another three-centre complex, composed of As_{Ga}, Ga_{As} and V_{Ga} (gallium vacancy), was proposed by Favero and Cruz [17] to account for the photoexcitation-induced transition of the EL2 defect from its normal to metastable configuration observed in their optical transmittance experiments. Two time constants revealed in those experiments have been attributed to two sequentially accessed metastable configurations of the complex.

On the other hand, Mohamed et al. [18] pointed to a similarity of the observed decrease in magnetization of the As_{Ga} spins with the normal to metastable state transition of EL2 defects. Their experimental results of temperature-dependent behaviour of magnetisation related to singly ionised charge state of As_{Ga} antisites in Be-doped GaAs layers, grown with low-temperature molecular-beam epitaxy, supported by first-principle calculations of the electron states of As_{Ga} antisites, suggested As_{Ga} as the origin of the EL2 defect. Very recent theoretical calculations by Wright and Modine [19] of the energy levels of isolated As_{Ga} antisites in GaAs, using newly developed bounds-analysis approach to interpret the density-functional-theory (DFT) results, are in very good agreement with the experimentally determined energy levels of the EL2 defects. Moreover, those calculations also show good agreement of the calculated activation energies of transformation of the As_{Ga} antisite from its interstitial configuration to the substitutional one with the experimental results for the transformation of the EL2 defects from their metastable to normal state.

The As_{Ga} defects act as double donors in GaAs giving rise to two deep energy levels in the band gap. As follows from the photo-EPR results [4], position of the single donor level (0/+) is at $E_C - 0.75$ eV and that of the double donor level (+/2+) at $E_V + 0.52$ eV, where E_C and E_V are the conduction and valence band edges, respectively. The single donor level was assigned to the EL2 electron trap, commonly revealed in DLTS experiments in n-type GaAs at a concentration of the order of 10^{16} cm^{-3}, displaying an electron-emission activation energy of 0.82 eV and a thermally activated electron capture cross-section with energy barrier of 66 meV [5, 20]. The double donor level of EL2 defect in the lower half of the band gap, giving rise to a hole trap in p-type GaAs, was revealed in few DLTS experiments only, mainly because of difficulties in preparing good-quality Schottky barrier diodes on p-type GaAs [21]. For the first time, this level was assigned by Lagowski et al. [21] to a DLTS peak, labelled by them as HM1, displaying a hole-emission activation energy of 0.52 eV. The thermal activation energy for a hole emission from this level of 0.54 eV was obtained from later investigations [20, 22–24].

In this article, we report on the results of systematic investigations of an electric-field enhancement of the thermal emission rate of holes from the trap attributed to the doubly ionised charge state of the defect responsible for EL2, measured with the DLTS technique in p-type GaAs Schottky barrier diodes prepared on various crystallographic surfaces of GaAs crystals. Partial results have already been published in a conference paper [23].

2 Samples and experimental methods Two kinds of p-type, Zn doped, liquid-encapsulated Czochralski (LEC) grown crystals with different shallow-acceptor concentrations, purchased from different sources, were investigated in order to obtain the emission rates over a large variation of the electric-field intensity. The room-temperature hole concentration was 5×10^{16} cm^{-3} in the crystal A and 1.4×10^{17} cm^{-3} in the crystal B. Schottky barrier diodes were prepared by Al and Au evaporation onto either of three main crystallographic surfaces, (100), (110) and (111) (As-terminated), of the samples cut from both crystals. Before evaporating, the samples were chemically polished and passivated in ammonium sulfide [25] in order to increase barrier height of the diodes. The diodes exhibited the barrier heights in the range from 0.75 to 0.80 V, as measured from both their capacitance versus voltage (C–V) and forward-bias current versus voltage (I–V) characteristics. DLTS measurements were performed under the conditions of leakage current density well below 1×10^{-4} A cm^{-2}, i.e. at the diode reverse bias up to 3 V, in order to exclude the impact-ionisation-induced enhancement of charge-carrier emission from deep levels [26].

Deep-level transient spectroscopy, developed by Lang [27], is a powerful and well-established technique for the investigation of electronic properties of deep-level defects in semiconductor materials and structures. It is based on the variation of the capacitance of a Schottky or p–n diode as a measure of the number of charge carriers trapped within its space-charge region during the filling pulse

applied to the reverse-biased diode. DLTS allows characterising and cataloguing deep levels by means of their capture cross-section and activation energy of thermal emission of charge carriers from the levels.

Additional information on the defect microscopic structure can be gained by applying external perturbation, such as uniaxial stress or strong electric field, during the DLTS experiment. The electric field, directed perpendicular to the plane of a Schottky or p–n junction, which exists in the space-charge region of the junction used for DLTS measurements, can be easily utilised to extend the standard DLTS technique. Strong electric field results in an enhancement of thermal emission rate of charge carriers from deep-level defects in the space-charge region in the direction of the field. In DLTS measurements, this effect causes a shift of the DLTS peak extremum towards lower temperatures and a decrease in the apparent activation energy of the corresponding deep level, while increasing the electric-field intensity. The magnitude of the influence of electric field on the emission rate strongly depends on the shape of the defect potential in the field direction. Thus, performing DLTS measurements under the electric field directed along various crystallographic axes enables to receive information on the local symmetry of defect potential [28].

We applied the so-called double-correlation DLTS (DDLTS) method [29], which allows for achieving well-defined intensity of the electric field in the observation window in the space-charge region of the reverse-biased diode. In this method, two filling pulse voltages of slightly different amplitudes, which define the narrow observation window in the space-charge region of a nearly constant electric field, are used to fill the trap levels. The difference of the capacitance transients resulting from thermal emission of charge-carriers from the traps, following each of the pulses, corresponds to the charge recovery for traps in the observation window only. For each of the investigated diodes the electric-field intensities in the observation window, determined by the used sequence of two voltage pulses, were calculated using the Schottky diode space-charge-region analysis described by Zotha and Watanabe [30] and taking into account the built-in voltages and hole concentrations received from C–V characteristics measured at various temperatures corresponding to the DDLTS-peak positions. The electric-field dependences of charge-carrier-emission rates from the investigated traps were obtained for various temperatures from DDLTS spectra recorded at three emission rate windows for each of the chosen electric-field intensity.

3 Experimental results and discussion The standard DLTS spectra measured for the two crystals at low electric fields are presented in Fig. 1. A trap corresponding to the hole emission from the doubly ionised charge state of the EL2 defect was the dominant deep-level trap revealed with DLTS in the both investigated crystals.

The trap concentrations in the crystals A and B were 6×10^{15} and $5 \times 10^{15}\,\mathrm{cm}^{-3}$, respectively. The temperature

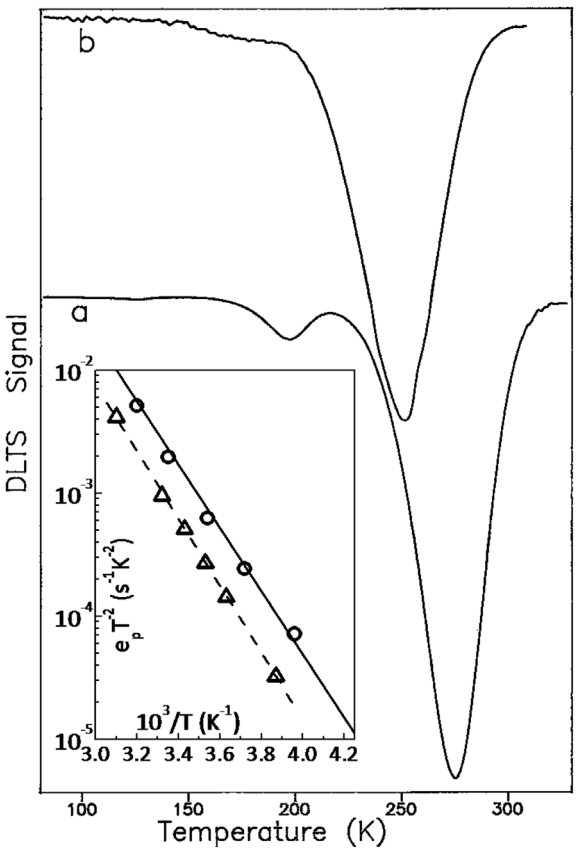

Figure 1 Hole-emission DLTS spectra measured at a rate window of $11\,\mathrm{s}^{-1}$ in (a) the crystal A at the electric field of $1 \times 10^5\,\mathrm{V\,cm}^{-1}$ and (b) the crystal B at the electric field of $1.5 \times 10^5\,\mathrm{V\,cm}^{-1}$. The dominant peak corresponds to the hole emission from the doubly ionised charge state of the EL2 defect. The inset shows temperature dependence of the thermal emission rates (Arrhenius plots) from the dominant traps revealed with DLTS in the crystal A (triangles) and crystal B (circles). The dashed line represents the Arrhenius plot fitted to the experimental points for the crystal A and the solid line represents the Arrhenius plot for the HM1 trap after [21].

dependences of the thermal emission rates (Arrhenius plots) from the trap in the two crystals are shown in the inset of Fig. 1. DLTS parameters of the trap, i.e. their apparent hole-emission activation energies and the capture cross-sections, evaluated from these dependences, are: $E_V + 0.54\,\mathrm{eV}$ and $\sigma_p = 8 \times 10^{-16}\,\mathrm{cm}^2$ for the crystal A and $E_V + 0.52\,\mathrm{eV}$ and $\sigma_p = 1 \times 10^{-15}\,\mathrm{cm}^2$ for the crystal B. Comparison with the literature data clearly confirms identification of the trap in the crystal B with the HM1 trap attributed to hole emission from the doubly ionised charge state of the EL2 defect by Lagowski et al. [21]. Larger activation energy of 0.54 eV, revealed for the trap in the crystal A with a smaller hole concentration, and thus measured at a lower electric-field intensity, was the same as those obtained from later experiments [20, 22].

Double-correlation DLTS spectra of the trap measured at various electric-field intensities in the crystal A, shown in Fig. 2, clearly evidence a strong influence of the electric

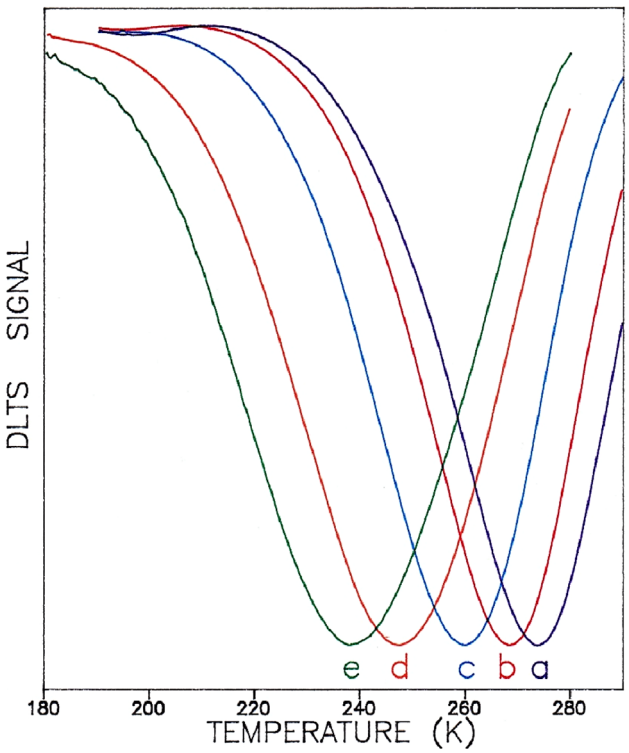

Figure 2 Double-correlation DLTS spectra of the doubly ionised charge state of the EL2 defect measured in the crystal A at the same rate window of $11\,s^{-1}$ and different electric-field intensities: $1.03 \times 10^5\,V\,cm^{-1}$ (a), $1.23 \times 10^5\,V\,cm^{-1}$ (b), $1.46 \times 10^5\,V\,cm^{-1}$ (c), $1.74 \times 10^5\,V\,cm^{-1}$ (d) and $1.90 \times 10^5\,V\,cm^{-1}$ (e).

field on the HM1 peak position, which shifts to lower temperatures with increasing field intensity. The peak position at the field of about $1.5 \times 10^5\,V\,cm^{-1}$ (Fig. 2c) is roughly the same as that measured with standard DLTS in the crystal B, shown in Fig. 1b.

In general, three mechanisms have been proposed to account for the electric-field-induced enhancement of the thermal emission rate of charge carriers from deep-level traps: the Poole–Frenkel effect, the phonon-assisted tunnelling and the direct tunnelling [31]. The latter mechanism becomes important only at very high electric-field intensities of the order of $10^7\,V\,cm^{-1}$, which are unattainable in our DLTS experiments, but the two former ones should be considered as responsible for the observed electric-field-induced shift of the DLTS HM1 peak. The classical Poole–Frenkel effect [32] describes the increase in the ionisation probability of charged traps in an external electric field as a result of the lowering of the barrier associated with their Coulomb potential. According to the one-dimensional Poole–Frenkel mechanism, the charge-carrier thermal emission rate e from a singly ionised trap with the attractive Coulomb potential increases exponentially with the square root of the electric-field intensity F as [31]:

$$e(F) = e(0)\exp(\beta\sqrt{F}/kT), \tag{1}$$

where $e(0)$ is the emission rate at zero electric field, $\beta = (q^3/\pi\varepsilon)^{1/2}$, q is the elementary charge, ε is the dielectric constant of the material, k is the Boltzmann constant and T is the absolute temperature.

Deep-level defects can be thermally ionised by multi-phonon processes if the energy of phonons is less than defect binding energy. Under a sufficiently strong electric field the defect ionisation probability can be significantly increased owing to the phonon-assisted tunnelling mechanism. Several theoretical treatments of this mechanism have been proposed. Makram-Ebeid and Lannoo [33] developed extensive numerical calculations in the quantum-mechanical approach. However, this rigorous quantum treatment does not provide with a simple analytical expression for the tunnel ionisation rate, which could be easily fitted to experimental results. Later on, Schenk [34, 35] derived approximate analytical expressions for electric-field-dependent multi-phonon emission by making a number of assumptions and simplifications in a detailed quantum-mechanical treatment. However, requirements for the accuracy of these expressions, which are likely valid for silicon, are not well satisfied for GaAs [36]. On the other hand, Karpus and Perel [37] proposed analytical solutions in a semi-classical theory of the phonon-assisted tunnelling mechanism. Here, we adopt the expressions obtained by Ganichev et al. [38, 39] within the adiabatic approximation based on the semi-classical theory by Karpus and Perel. In this approximation, the charge-carrier thermal emission rate from a deep-level defect increases exponentially with the square of the electric-field intensity as

$$e(F) = e(0)\exp\left(F^2/F_c^2\right), \tag{2}$$

where $F_c = \sqrt{3m^*\hbar/\tau_2^3 q^2}$ is the characteristic field intensity, m^* is the effective mass of charge carriers, $\hbar$ is the Planck constant divided by 2π and τ_2 is the tunnelling time, given by [38]

$$\tau_2 = \hbar/2kT \pm \tau_1, \tag{3}$$

where the time constant τ_1 is of the order of the inverse local defect vibration frequency and the plus and minus signs refer to the adiabatic potential structures of substitutional (moderate lattice relaxation) and autolocalised (very large lattice relaxation leading to a metastable behaviour) defects, respectively.

The DDLTS results of the hole-emission rates from the doubly ionised charge state of the EL2 defect, obtained at various temperatures for the electric field applied perpendicular to each of the three main crystallographic surfaces of the crystal A, plotted as a function of square root of the electric-field intensity, are shown in Fig. 3. Similar dependences revealed for the field directions parallel to the three main crystallographic axes indicate tetrahedral local symmetry of the EL2 defect being in the doubly ionised charge state. The dashed line in Fig. 3 represents an enhancement of the hole-emission rate with the electric-field

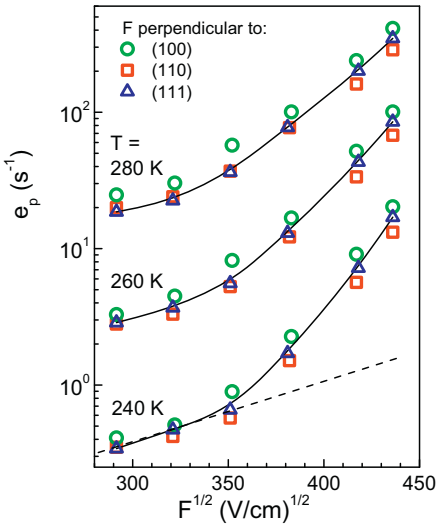

Figure 3 Dependences of the hole-emission rates from the doubly ionised charge state of the EL2 defect on square root of the electric-field intensity at various temperatures, measured in the samples of different orientations, written in the figure, cut from the crystal A. The dashed line represents an electric-field enhancement of emission rate according to the classical Poole–Frenkel mechanism. The solid lines act as a guide to the eye.

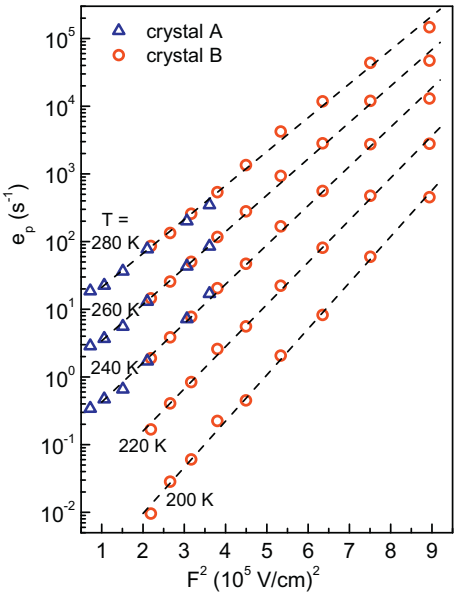

Figure 4 Dependences of the hole-emission rates from the doubly ionised charge state of the EL2 defect on square of the electric-field intensity at various temperatures, measured in the samples cut parallel to the (111) surface from the crystal A (triangles) and crystal B (circles). The dashed lines represent the phonon-assisted tunnelling mechanism of ionisation fitted to the experimental points.

intensity as predicted by the classical Poole–Frenkel effect calculated for a single acceptor trap with the attractive Coulombic potential, as described by Eq. (1). In the case of hole emission from a doubly ionised donor, which occurs in the experiment, repulsive Coulombic interaction between the emitted hole and the positively charged trap would result in a still weaker electric-field dependence of the emission rate. On the contrary, as appears from Fig. 3, the measured hole-emission rates reveal, for the electric-field intensities larger than about 1×10^5 V cm^{-1} ($\sqrt{F} > 330$ (V cm^{-1})$^{1/2}$), a much stronger field dependence thus pointing to a phonon-assisted tunnelling of holes from the deep-level trap to the valence band.

The experimental results for the two investigated crystals, covering much broader range of the electric-field intensity, plotted as a function of square of the electric-field intensity, are presented in Fig. 4. They show an enhancement of the hole-emission rate by over four orders of magnitude for the threefold increase in the electric-field intensity. At the electric-field intensities larger than 1×10^5 V cm^{-1} this enhancement follows the relation $\ln[e(F)] \propto F^2$, described by Eq. (2), characteristic of the phonon-assisted tunnelling mechanism. Fitting Eq. (2) to the experimental results for $F > 1 \times 10^5$ V cm^{-1}, shown with the dashed lines in Fig. 4, provides with the characteristic field intensity values F_c. From the F_c values, obtained for various temperatures from the slope of $\ln[e(F)]$ as a function of F^2, we have determined the tunnelling times τ_2. They are plotted in Fig. 5 as a function of inverse temperature showing linear dependence as predicted by Eq. (3). Fitting that equation to the τ_2 values requires an additional fitting parameter α (close to unity) and the plus sign in Eq. (3), according to the following relation [40]:

$$\tau_2 = \alpha\hbar/2kT + \tau_1, \tag{4}$$

which gives the τ_1 value equal to 2.9×10^{-14} s. This value of τ_1 time constant is an order of magnitude larger than the τ_1 values determined previously for two electron traps, called EL3 and EL5, associated with defects of lowered local symmetry in n-type GaAs crystals [40] and for the DX centre in Te-doped n-type AlGaAs ternary compound [39].

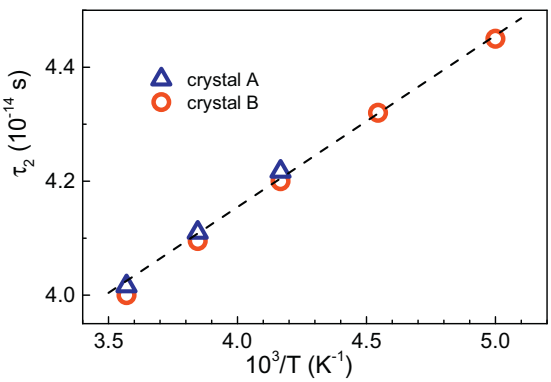

Figure 5 Tunnelling times τ_2, calculated from fitting Eq. (2) to the results obtained for the crystal A (triangles) and crystal B (circles) as a function of inverse temperature. The dashed line represents fitting Eq. (4) to the results with the fitting parameter $\alpha = 0.79$ and $\tau_1 = 2.9 \times 10^{-14}$ s.

On the other hand, two to three times larger τ_1 values, of above 5×10^{-14} s, have been obtained for deep-level traps associated with substitutional Au and Hg impurities in p-type Ge [41] and the vacancy-oxygen complexes in n-type Ge [42].

The plus sign in Eq. (3), determined from best fitting the revealed electric-field and temperature dependence of the emission rate of holes from the HM1 traps with theoretical predictions of the phonon-assisted tunnelling mechanism, points to a substitutional type of adiabatic potential structure, with a moderate lattice relaxation, of the defect responsible for the traps. For this type adiabatic potential, the τ_1 time constant is described by the following relation [38]:

$$\tau_1 = (2\omega)^{-1} \ln(E_T/d_{FC}), \quad (5)$$

where ω is the local defect vibration frequency, E_T is the defect thermal ionisation energy and d_{FC} is the Franck–Condon shift between optical and thermal ionisation energies of the deep-level defect, which is proportional to the strength of the defect coupling to the lattice. The Franck–Condon shift can be written as: $d_{FC} = S\hbar\omega$, where $\hbar\omega$ is the energy of a local phonon coupled to the defect and S is the Huang–Rhys factor, which represents the average number of phonons created during the lattice relaxation accompanied the defect ionisation [43].

In our previous article [23], we have analysed the obtained results of electric-field and temperature dependences of hole-emission rates from the doubly ionised charge state of the EL2 defect within the quantum-mechanical approach by Makram-Ebeid and Lannoo [33]. From fitting the theoretical curves to our experimental results we have obtained the value of the Franck–Condon shift $S\hbar\omega \approx 180$ meV [23]. Introducing this value to Eq. (5) and taking $E_T = 0.52$ eV, we get the local defect vibration frequency $\omega \approx 1.8 \times 10^{13}\ s^{-1}$ and thus the phonon energy $\hbar\omega \approx 12$ meV and the Huang–Rhys factor $S \approx 15$. Although these results are comparable with the values of $\hbar\omega \approx 20$ meV and $S\hbar\omega \approx 140$ meV, reported in Ref. [33] for the electron emission from the single donor level of the EL2 defect in n-type GaAs, their comparison suggests a distinctly softer lattice relaxation around the defect in the doubly ionised charge state with respect to that in the singly ionised charge state of the EL2 defect.

4 Conclusions Very strong electric-field-induced enhancement of the thermal emission rate of holes from the double donor level of the EL2 defect, by over four orders of magnitude of the emission rate, was observed in p-type GaAs. The effect can be described using the semi-classical theory of the phonon-assisted tunnel emission with a moderate coupling of the defect to the lattice vibronic modes. Fitting the experimental results to the theory yields the Franck–Condon shift of the defect of about 180 meV and the Huang–Rhys factor equal to 15. The fact that the effect was the same when measured at the field directions parallel to the three main crystallographic axes provides an argument for tetrahedral symmetry of the EL2 defect, which is consistent with the defect identification as the isolated As antisite.

Acknowledgements The author would like to dedicate this article to the memory of A. Makosa, who initiated and actively participated in the reported research before his untimely death. He is also very grateful to J. Z. Domagala for X-ray orientation of the investigated crystals.

References

[1] J. A. del Alamo, Nature **479**, 317 (2011).
[2] H.-P. Komsa and A. Pasquarello, J. Phys.: Condens. Matter **24**, 045801 (2012).
[3] A. Stesmans, S. Nguyen, and V. V. Afanas'ev, Appl. Phys. Lett. **103**, 162111 (2013).
[4] E. R. Weber, H. Ennen, U. Kaufmann, J. Windscheif, J. Schneider, and T. Wosinski, J. Appl. Phys. **53**, 6140 (1982).
[5] J. Lagowski, H. C. Gatos, J. M. Parsey, K. Wada, M. Kaminska., and W. Walukiewicz, Appl. Phys. Lett. **40**, 342 (1982).
[6] T. Figielski, E. Kaczmarek, and T. Wosinski, Appl. Phys. A **38**, 253 (1985).
[7] T. Figielski and T. Wosinski, Phys. Rev. B **36**, 1269 (1987).
[8] P. Trautman, J. P. Walczak, and J. M. Baranowski, Phys. Rev. B **41**, 3074 (1990).
[9] B. K. Meyer, D. M. Hofmann, and J.-M. Spaeth, Mater. Sci. Forum **10–12**, 311 (1986).
[10] B. K. Meyer, D. M. Hofmann, J. R. Niklas, and J. M. Spaeth, Phys. Rev. B **36**, 1332 (1987).
[11] H. J. von Bardeleben, D. Stievenard, D. Deresmes, A. Huber, and J. C. Burgoin, Phys. Rev. B **34**, 7192 (1986).
[12] T. Wosinski, Semicond. Sci. Technol. **3**, 411 (1988).
[13] T. Wosinski, A. Makosa, and Z. Witczak, Semicond. Sci. Technol. **9**, 2047 (1994).
[14] F. K. Koschnick and J.-M. Spaeth, Phys. Status Solidi B **216**, 817 (1999).
[15] A. Fukuyama, T. Ikari, Y. Akashi, and M. Suemitsu, Phys. Rev. B **67**, 113202 (2003).
[16] D. Kabiraj and S. Ghosh, Appl. Phys. Lett. **87**, 252118 (2005).
[17] P. P. Favero and J. M. R. Cruz, Eur. Phys. J. B **47**, 363 (2005).
[18] M. A. Mohamed, P. T. Lam, K. W. Bae, and N. Otsuka, J. Appl. Phys. **110**, 123716 (2011).
[19] A. F. Wright and N. A. Modine, Phys. Rev. B **91**, 014110 (2015).
[20] M. Hoinkis, E. R. Weber, W. Walukiewicz, J. Lagowski, M. Matsui, H. C. Gatos, B. K. Meyer, and J. M. Spaeth, Phys. Rev. B **39**, 5538 (1989).
[21] J. Lagowski, D. G. Lin, T.-P. Chen, M. Skowronski, and H. C. Gatos, Appl. Phys. Lett. **47**, 929 (1985).
[22] G. A. Samara, D. W. Vook, and J. F. Gibbons, Phys. Rev. Lett. **68**, 1582 (1992).
[23] A. Makosa, T. Wosinski, and W. Szkielko, Acta Phys. Polon. A **82**, 813 (1992).
[24] N. A. Naz, U. S. Quarashi, and M. Z. Iqbal, J. Appl. Phys. **106**, 103704 (2009).
[25] M. S. Carpenter, M. R. Melloch, and T. E. Dungan, Appl. Phys. Lett. **53**, 66 (1988).

[26] J. Lagowski, D. G. Lin, H. C. Gatos, J. M. Parsey, and M. Kaminska, Appl. Phys. Lett. **45**, 89 (1984).
[27] D. V. Lang, J. Appl. Phys. **45**, 3023 (1974).
[28] A. Mircea and A. Mitonneau, J. Physique Lett. **40**, L-31 (1979).
[29] H. Lefevre and M. Schulz, Appl. Phys. **12**, 45 (1977).
[30] Y. Zotha and M. O. Watanabe, J. Appl. Phys. **53**, 1809 (1982).
[31] J. Bourgoin and M. Lannoo, Point Defects in Semiconductors II, Experimental Aspects (Springer, Berlin, 1983).
[32] J. Frenkel, Phys. Rev. **54**, 657 (1938).
[33] S. Makram-Ebeid and M. Lannoo, Phys. Rev. B **25**, 6406 (1982).
[34] A. Schenk, J. Appl. Phys. **71**, 3339 (1992).
[35] A. Schenk, Solid State Electron. **35**, 1585 (1992).
[36] R. M. Fleming, S. M. Myers, W. R. Wampler, D. V. Lang, C. H. Seager, and J. M. Campbell, J. Appl. Phys. **116**, 013710 (2014).
[37] V. Karpus and V. I. Perel, Zh. Eksper. Teor. Fiz. **91**, 2319 (1986) [Sov. Phys. JETP **64**, 1376 (1986)].
[38] S. D. Ganichev, I. N. Yassievich, and W. Prettl, Fiz. Tverd. Tela **39**, 1905 (1997) [Phys. Solid State **39**, 1703 (1997)].
[39] S. D. Ganichev, E. Ziemann, W. Prettl, I. N. Yassievich, A. A. Istratov, and E. R. Weber, Phys. Rev. B **61**, 10361 (2000).
[40] T. Tsarova, T. Wosinski, A. Makosa, and Z. Tkaczyk, Semicond. Sci. Technol. **24**, 105021 (2009).
[41] S. D. Ganichev, W. Prettl, and P. G. Huggard, Phys. Rev. Lett. **71**, 3882 (1993).
[42] V. P. Markevich, A. R. Peaker, V. V. Litvinov, L. I. Murin, and N. V. Abrosimov, Physica B **376–377**, 200 (2006).
[43] K. Huang and A. Rhys, Proc. Roy. Soc. London A **204**, 406 (1950).

